

# Influence of lubricant filling on the dry sliding wear behaviors of hybrid PTFE/Nomex fabric composite

Guina Ren · Zhaozhu Zhang · Xiaotao Zhu ·  
Xuehu Men · Weimin Liu

Received: 28 October 2013 / Accepted: 23 January 2014 / Published online: 12 February 2014  
© Springer Science+Business Media New York 2014

**Abstract** To improve the antiwear property and load carrying capacity of hybrid PTFE/Nomex fabric/phenolic composites, graphene and graphene oxide (GO) had been synthesized and were employed as fillers, together with graphite. Sliding wear tests show that the wear rates of filler-reinforced PTFE/Nomex fabric composites were reduced greatly when compared to unfilled fabric composite. Besides, it was found that the 2 wt% GO filled PTFE/Nomex fabric composites exhibited the optimal tribological properties. It was proposed that the self-lubrication of GO, the favorable interface stability of the composite, and the uniform transfer film on the counterpart pin contributed together to the reinforced tribological property of GO filled PTFE/Nomex fabric composite. We also investigated the influence of filler content, applied load, sliding speed, and tensile and bonding strength on the tribological properties of PTFE/Nomex fabric composites.

## Introduction

Hybrid fabric composites have recently generated extensive interests owing to their outstanding properties, such as self-lubricating, low density, high strength, and wide performance tailorability [1–3]. The self-lubrication of PTFE fiber and the high strength and thermal and oxidative

stability of Nomex fiber endow PTFE/Nomex hybrid fabric composite with excellent practicability [4, 5]. To take full advantage of hybrid PTFE/Nomex fabric composite, the face of the hybrid fabric rich in PTFE fiber was subjected to wear due to its low friction property, while the other face rich in Nomex fiber adhered onto the substrate. However, the invalidation of hybrid PTFE/Nomex fabric composite will always be accelerated due to the poor antiwear property of PTFE fiber and the weak bonding between fabric and adhesive [6–8]. As a consequence, it is an urgent demand to improve the antiwear property of the hybrid PTFE/Nomex fabric composites.

Surface modifications of fabric and filler reinforcing are the two universal ways of improving the tribological properties of fabric composites which can be applied either individually or corporately [9–11]. Surface modifications can change the surface morphology and reactivity of the fiber, which lead to an improvement in the bonding strength between fabric and adhesive, and thus improve the tribological properties of fabric composite [12, 13]. Besides, the incorporation of lubricants or nanoparticles into fabric composites has also shown tremendous promise in achieving longevity and the desired tribological properties [14, 15]. Graphite, graphene, and graphene oxide (GO) have been proved to be effective lubricant fillers for polymer composites including fabric composites [16, 17]. Especially, GO possesses high specific surface, good dispersibility in water and organic solvents, and ideal range of reactive surface-bound functional groups, and these desired properties promote the interaction between the fillers and the polymers [18]. For example, Wan and Chen [19] reported that GO reinforced PLLA, PCL, PS, and PE composites showed improved mechanical and tribological property when compared to the unfilled one. Thus, GO reinforced PTFE/Nomex fabric composite was expected to

---

G. Ren · Z. Zhang (✉) · X. Zhu · X. Men · W. Liu  
State Key Laboratory of Solid Lubrication, Lanzhou Institute of  
Chemical Physics, Chinese Academy of Sciences, Tianshui Road  
18th, Lanzhou 730000, People's Republic of China  
e-mail: zzzhang@licp.cas.cn

G. Ren  
University of Chinese Academy of Sciences, Beijing 100039,  
People's Republic of China

show a stable interface and favorable mechanical and tribological properties.

In this study, we employed GO, graphite, and graphene as fillers to improve the tribological property of PTFE/Nomex hybrid fabric composite. Wear tests showed that the tribological properties of these three fillers reinforced fabric/phenolic composites were optimized, when compared with unfilled fabric composite. We also investigated the effects of filler content, applied load, and sliding speed on the tribological properties of the hybrid PTFE/Nomex fabric composites. Based on the characterizations, the probable reasons for the reinforcement were discussed. This study is hoped to extend the application of fabric composite.

## Experimental

### Materials

The satin-weave hybrid PTFE/Nomex fabric was woven out of the PTFE fibers and Nomex fibers purchased from DuPont Plant. The adhesive resin (204 phenolic resin) was provided by Shanghai Xing-guang Chemical Plant, China. The graphite (diameter in the range of 10–38  $\mu\text{m}$  determined by scanning electron microscopy, SEM analysis) was provided by Lanshu Graphite Plant, China. The rest chemicals were all of analytical grade and used as received.

### Preparation of graphene and GO

Typically, GO was synthesized from natural graphite powder by a modified Hummers method [20, 21]. 5 g graphite powder was added into 120 mL cooled (0  $^{\circ}\text{C}$ ) concentrated  $\text{H}_2\text{SO}_4$ , and 15 g  $\text{KMnO}_4$  was added into this solution under stirring and cooling for 30 min (the temperature of this mixture was kept below 20  $^{\circ}\text{C}$ ). Then, the mixture was stirred at 35  $^{\circ}\text{C}$  for 120 min, and 230 mL distilled water was slowly added to the solution to cause the temperature increased to 98  $^{\circ}\text{C}$ . The reaction was terminated by adding 700 mL distilled water and 20 mL 30 %  $\text{H}_2\text{O}_2$  solution. The resulting brilliant yellow mixture product was washed with 5 %  $\text{HCl}$  solution repeatedly until sulfate could not be detected with  $\text{BaCl}_2$  and then washed with distilled water to remove the acid. Exfoliation was carried out by sonicating distilled water diluted GO dispersion for 60 min.

Then, part of the suspension was dried in a vacuum oven at 60  $^{\circ}\text{C}$  for 24 h to obtain GO nanosheets. And the rest mixture was reduced with superfluous hydrazine hydrate ( $\text{N}_2\text{H}_4\cdot\text{H}_2\text{O}$ ) at 80  $^{\circ}\text{C}$  for 24 h. After reduction, a homogeneous black dispersion with a small amount of black precipitate was obtained. Finally, the suspension was dried

in a vacuum oven at 60  $^{\circ}\text{C}$  for 24 h to obtain graphene nanosheets.

### Specimen preparation

The hybrid PTFE/Nomex fabric was cleaned by Soxhlet extractor in petroleum ether and ethanol in sequence and dried at 80  $^{\circ}\text{C}$ . Then the fillers were mixed evenly with the phenolic resin (diluted with mixed solvent  $V_{\text{ethanol}}:V_{\text{acetone}}:V_{\text{ethyl acetate}} = 1:1:1$ ) at different mass fractions under magnetic stirring and ultrasonic stirring. Afterwards, the fabric was immersed in the pure or filler added adhesive solution and dried at 45–50  $^{\circ}\text{C}$ . Repetitive immersions and coatings of the fabric were performed to obtain the composite in which the mass fraction of the fabric was about 70–75 %. Finally, a series of unfilled and lubricants filled fabric composites were affixed onto the AISI-1045 steel (size of  $\Phi 45 \text{ mm} \times 8 \text{ mm}$ , surface roughness of 0.45  $\mu\text{m}$ ) with the adhesive resin and then cured at 180  $^{\circ}\text{C}$  for 2 h under a certain pressure.

### Tensile and bonding strength test

The tensile and bonding strength of pure and 4 % filler reinforced hybrid PTFE/Nomex fabric composites were determined by a DY35 universal materials test machine at a constant speed of 50 mm/min. The dimensions of the sample used for tensile strength test were 100 mm in length, 20 mm in width, and  $624 \pm 20 \mu\text{m}$  in thickness. The tensile strength  $\sigma_b$  (MPa)

$$\sigma_b = F_p(BD)^{-1},$$

where  $F_p$  is the maximal pull force in N,  $B$  is the width in m, and  $D$  is the thickness in m.

Before carrying out the bonding property tests, the impregnated fabric was cut into pieces (20 mm in length and 12 mm in width). After that, the test pieces were affixed between two AISI-1045 steel plates with the adhesive resin and then cured at 180  $^{\circ}\text{C}$  for 2 h under a certain pressure. The bonding strength  $\tau$  (MPa)

$$\tau = F(LB)^{-1},$$

where  $F$  is the maximal pull force in N,  $B$  is the width in m, and  $L$  is the length in m. Each experiment was carried out five times and the average value was used.

### Friction and wear test

Sliding wear tests were performed in a Xuanwu-III pin-on-disk tribometer, according to our previous work [22]. In the pin-on-disk tester, a stationary steel pin slides against the Nomex fabric composite specimen in a rotating steel disk. The flat-ended AISI-1045 pin (diameter 2 mm) was

secured to the load arm with a chuck. The distance between the center of the pin and the axis was 12.5 mm. The pin stays over the disk with two degrees of freedom: a vertical one, for normal load application by direct contact with the disk, and a horizontal one, for friction measurement.

To make the surface roughness  $R_a$  of the pin at about  $0.15\ \mu\text{m}$ , it was polished with 350, 700, and 900 grade waterproof abrasive papers in sequence before each test and then the polished pin was cleaned with acetone. The dry sliding wear tests were performed on the Xuanwu-III pin-on-disk tribometer at room temperature for 2 h, with the loads and speeds in the range of 65–115 MPa and 0.364–0.572 m/s, respectively. After each test, the corresponding wear volume loss ( $V$ ) of the composite was acquired by measuring the depth of the wear scar on a micrometer with the resolution of 0.001 mm. The wear performance was expressed by wear rate ( $\omega$ ,  $\text{m}^3/\text{N}/\text{m}$ ) as follows:  $\omega = V * (PL)^{-1}$ , where  $V$  is the wear volume loss in  $\text{m}^3$ ,  $P$  is the load in N, and  $L$  is the sliding distance in m.

The friction coefficient which was measured from the frictional torque gained by a load cell sensor could be obtained from the computer running the friction measure software. The contact temperature of the worn surface was monitored by a thermocouple positioned at the edge of the counterpart pin. Each experiment was carried out three times and the average value was used.

## Characterization

FEI Tecnai F30 transmission electron microscopy (TEM) and Bruker IFS66/S Fourier transform infrared (FTIR)

spectrometer were employed to investigate the morphology and microstructure of graphene and GO. X-ray power diffraction (XRD) patterns were obtained using a D/Max-2400 X-ray diffractometer. SEM (JSM-5600LV) was used to observe the worn surface morphology of the fabric composites and the pins.

## Results and discussion

### Characterization of graphene, GO, and graphite

Figure 1a–c shows the TEM images of graphene, GO, and graphite, in which the graphitic lattice is clearly illustrated. And it can be seen that graphene exhibits a broad diffraction peak at around  $23.9^\circ$  (see Fig. 1d) and graphite exhibits an intense diffraction peak at around  $26^\circ$  (see Fig. 1f) [23]. The diffraction peak positioned at  $2\theta$  around  $10.0^\circ$  for GO (see Fig. 1e) indicating that many oxygen atoms were introduced into the interplanar space and planar surface of graphite [23].

Figure 1g shows the FTIR spectra of graphene, GO, and graphite. For graphene, GO, and graphite, the absorption band at  $3400\ \text{cm}^{-1}$  is attributed to C–OH and the band at  $1620\ \text{cm}^{-1}$  to aromatic C=C [24, 25]. As for graphene and graphite, the band at  $1019\ \text{cm}^{-1}$  is attributed to the C–O vibrations of the epoxy groups [24]. Furthermore, the peaks of GO positioned at  $1724$ ,  $1224$ ,  $1052$ , and  $848\ \text{cm}^{-1}$  are attributed to C=O stretching vibrations from carbonyl groups, carboxylic groups, C–OH stretching, and C–O vibrations of the epoxy groups, respectively [25]. The

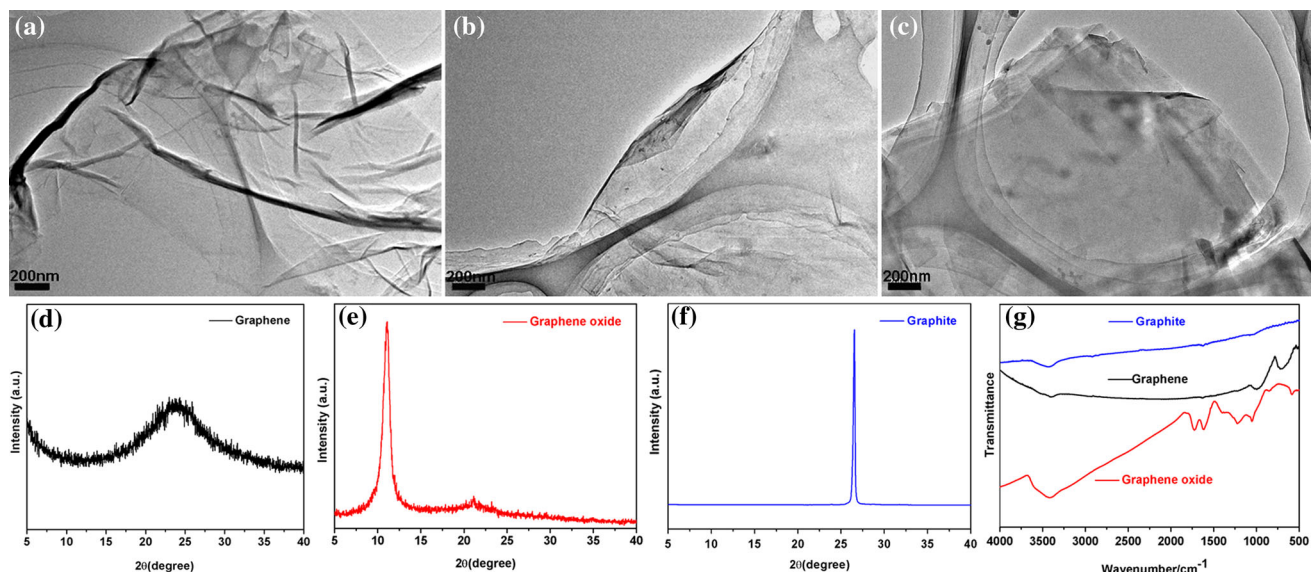


**Fig. 1** TEM images of the graphene (a), graphene oxide (b), and graphite (c), XRD pattern of graphene (d), graphene oxide (e), and graphite (f). (g) FTIR spectra of graphene, graphene oxide, and graphite

results of XRD and FTIR analysis indicated that graphene and GO have been successfully synthesized.

The mechanical and tribological property of unfilled and filler reinforced hybrid fabric composite

To investigate the influence of filler content on the tribological properties of the hybrid fabric composite, sliding wear tests were carried out. Figure 2a, b shows the friction coefficient and wear rate of unfilled and a series of lubricant filled fabric composites. It can be seen that the friction coefficient of lubricant reinforced composite varied little with the filler content. However, the wear rates of the most lubricant reinforced fabric composites were reduced in different extent. For all the lubricants reinforced fabric composites, the wear rate decreased initially and then increased with the filler content. When graphite was employed as filler, 2 and 4 wt% graphite reinforced hybrid fabric composites showed lower wear rate than unfilled composite, while the 6 and 8 wt% graphite reinforced composite showed higher wear rate. Among the graphite

filled hybrid fabric composites investigated, 4 wt% graphite filled hybrid fabric composites displayed the most admirable antiwear property. When graphene and GO were used as fillers at the content of 1–8 wt%, all the fillers reinforced composites exhibited lower wear rates than that of the pure composite. The optimal filler content for both graphene and GO is 2 wt%. Moreover, GO reinforced fabric composite showed better antiwear property than graphene reinforced composite when the same content was applied.

We then investigated the tensile and bonding strength of pure and 4 wt% fillers reinforced composites (see Fig. 2c). It was found that the tensile and bonding strength of fabric composite followed the order of unfilled fabric composite > GO filled fabric composite > graphite filled fabric composite > graphene filled fabric composite. For filler-reinforced composites, the stronger the mechanical property, the better the antiwear property. Liu et al. [26] investigated the influence of PTFE volume content on the mechanical and tribological properties of aramid fabric reinforced PTFE composites. And they found that the

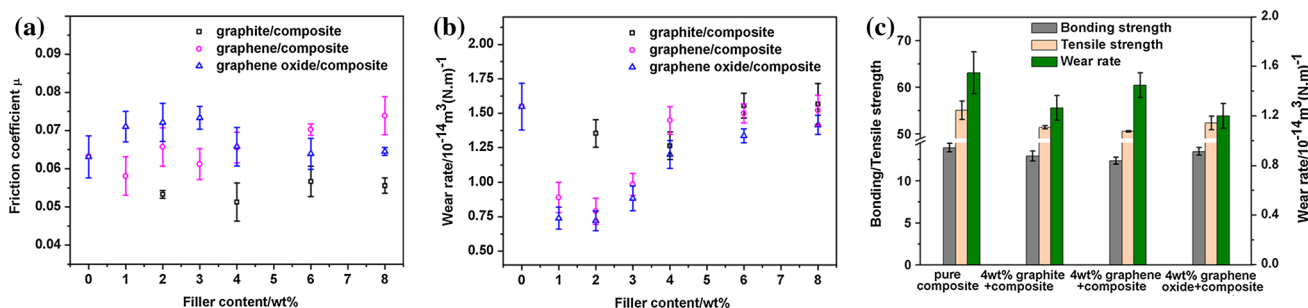


**Fig. 2** The value of friction coefficient (a) and wear rate (b) of the fabric composite as a function of filler content. The load and sliding speed in the tests were 85 MPa and 0.364 m/s, respectively, (c) the tensile and bonding strength and wear rate of several fabric composites

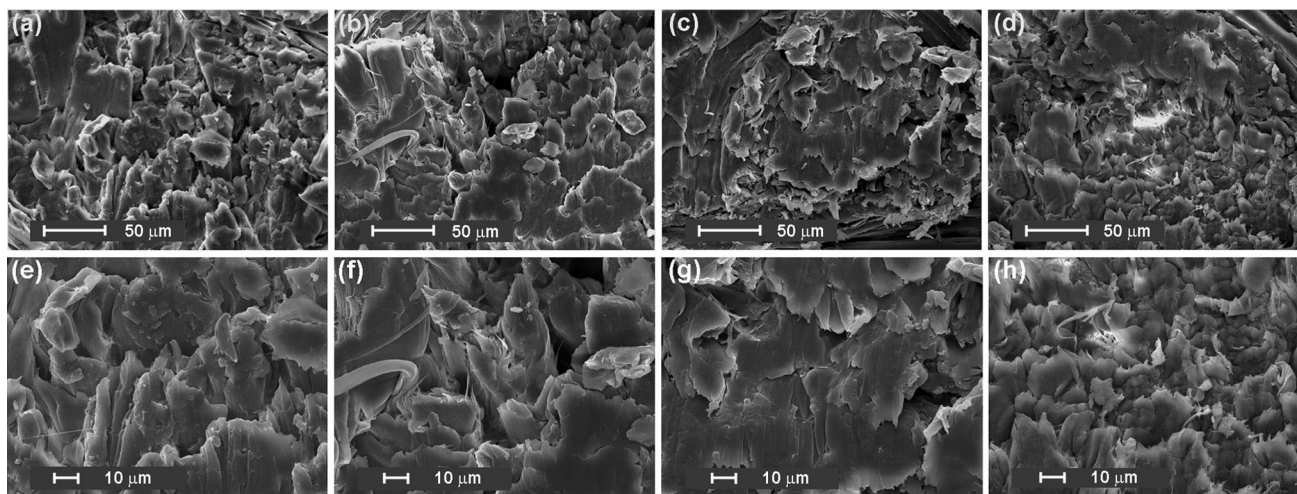


**Fig. 3** SEM images of the fracture surfaces of a unfilled fabric composite, b 4 wt% graphite filled fabric composite, c 4 wt% graphene filled fabric composite, and d 4 wt% graphene oxide filled fabric composite, e–h magnified images of a–d, respectively

composite possessed the highest tensile strength and the highest Rockwell hardness exhibited the lowest friction coefficient and the best wear resistance. The results of our tests together with the investigation of Liu et al. approved the fact that the mechanical property and tribological property of composites are closely related to each other.

The fracture surfaces of unfilled and filler-reinforced composites are shown in Fig. 3. It can be seen from Fig. 3a, e that the interfacial bonding is compact for unfilled composite. However, for graphite and graphene reinforced fabric composites, some holes were detected on the fracture surfaces of the composites (Fig. 3b, c, f, g). For GO reinforced fabric composite, the interfacial bonding is equally compact without any hole and void (see Fig. 3d, h), compared to unfilled composite. Thus, GO reinforced fabric composite displayed improved tensile and bonding strength, compared to graphite and graphene reinforced fabric composites. It is proposed that fabric composite with higher tensile and bonding strength will be difficult undergoing damages such as resin shell-off and fiber

pull-out. Accordingly, the integrated structure of GO reinforced fabric composite contributed to its optimal antiwear property and load carrying capacity.

The effect of applied load on the tribological properties of the composite

Subsequently, the effect of applied load on the friction and wear behaviors of unfilled and GO filled fabric composites were investigated, and the result was shown in Fig. 4. It can be seen that the friction coefficients of these two fabric composites decreased with the applied load increasing, accompanied with an increase in the wear rate simultaneously. The friction coefficient of GO filled composite was lower initially but become higher than the unfilled composite with the applied load (see Fig. 4a). It was proposed that exposed PTFE fibers were less during the sliding wear test for GO reinforced composite and thus it exhibited a higher friction coefficient when compared with unfilled composite. The wear rate of GO filled composite was much

**Fig. 4** Friction coefficient (a) and wear rate (b) of unfilled and graphene oxide filled hybrid fabric composite as a function of applied load. The sliding speed in the tests was 0.364 m/s

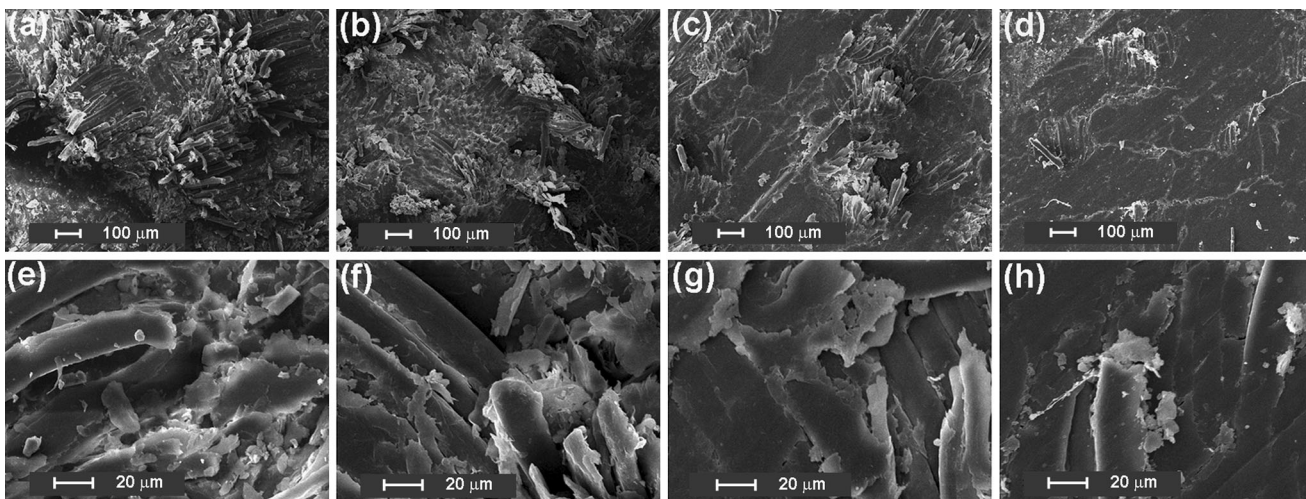
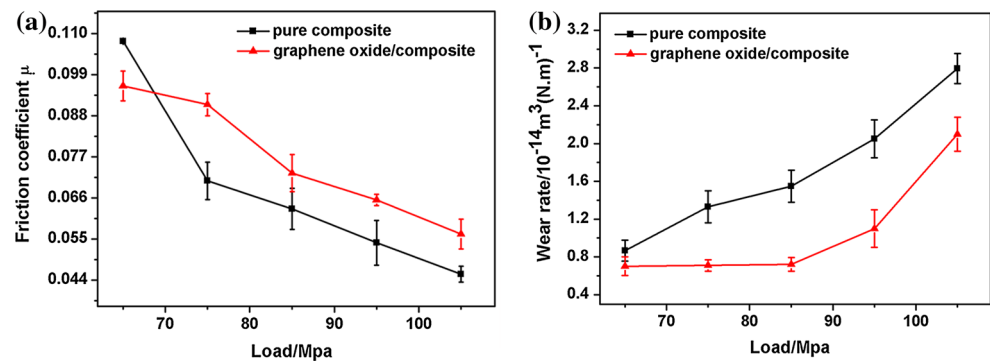


**Fig. 5** SEM images of the worn surfaces for **a** unfilled fabric composite, **b** 4 wt% graphite filled fabric composite, **c** 2 wt% graphene filled fabric composite, and **d** 2 wt% graphene oxide filled

fabric composite, **e–h** magnified images of **a–d**, respectively. The applied load and sliding speed in the tests were 85 MPa and 0.364 m/s, respectively

**Fig. 6** The transfer films formed on the counterpart pin after the sliding wear tests for unfilled composite (a), 4 wt% graphite filled composite (b), 2 wt% graphene filled composite (c), and 2 wt% graphene oxide filled composite (d). The applied load and sliding speed in the tests were 85 MPa and 0.364 m/s, respectively

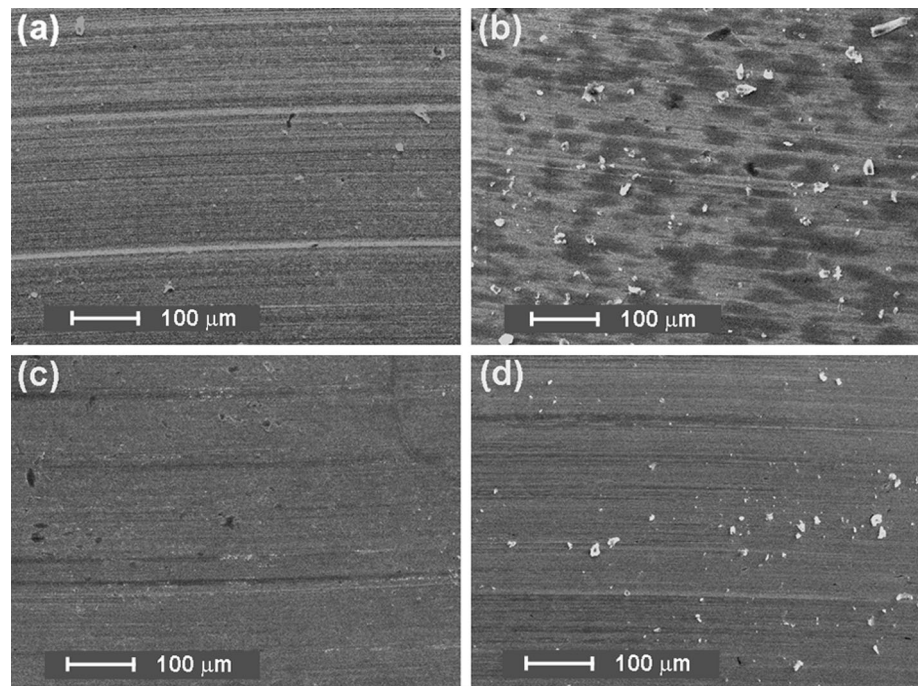
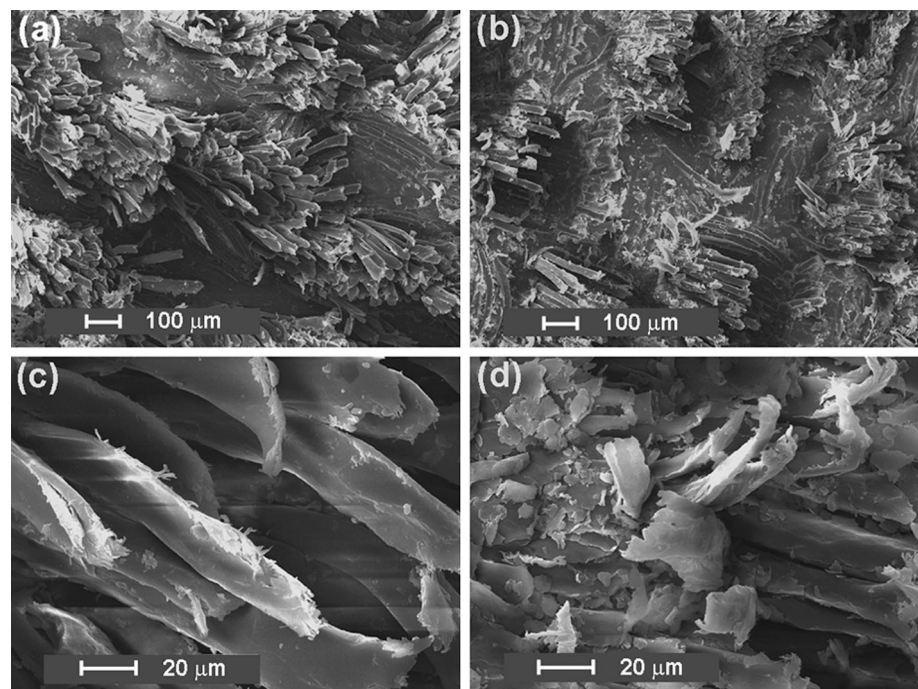


**Fig. 7** SEM images of the worn surfaces for a unfilled composite and b graphene oxide filled composite, c, d magnified images of a, b, respectively. The applied load and sliding speed in the tests were 105 MPa and 0.364 m/s, respectively



lower than that of unfilled composite under all the investigated applied loads (see Fig. 4b). That is, the load carrying capacity and antiwear property of fabric composite were notably improved after filling 2 wt% GO. It is likely that the evenly distributed GO nanosheets can share the applied load effectively and thus the damage caused by shear force was weakened [27].

Figures 5 and 6 show the morphology of the worn surfaces and its counterpart pins of unfilled, 4 wt% graphite filled, 2 wt% graphene filled, and 2 wt% GO filled fabric composites. It can be seen that large area of adhesive detached on the worn surface of unfilled fabric composite, and bundles of fibers were cut off from the composite (see Fig. 5a, e), indicating severe adhesive wear and fatigue

**Fig. 8** The effect of sliding speed on the friction coefficient (a) and wear rate (b) for unfilled and graphene oxide filled fabric composite. The applied load in the tests was 85 MPa

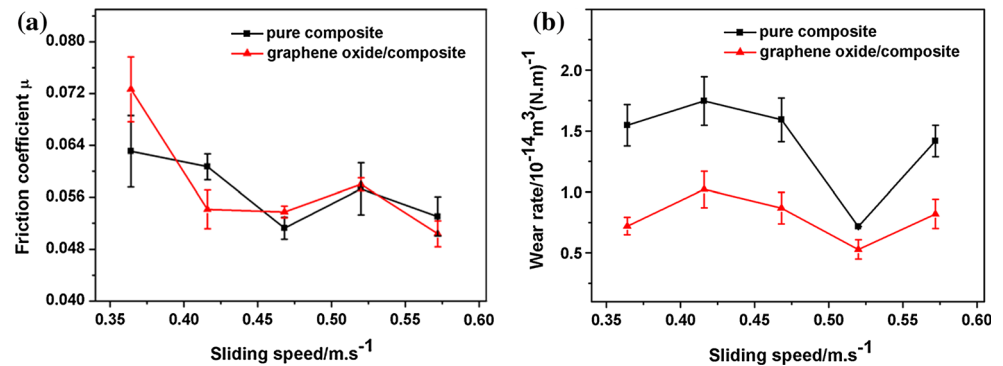
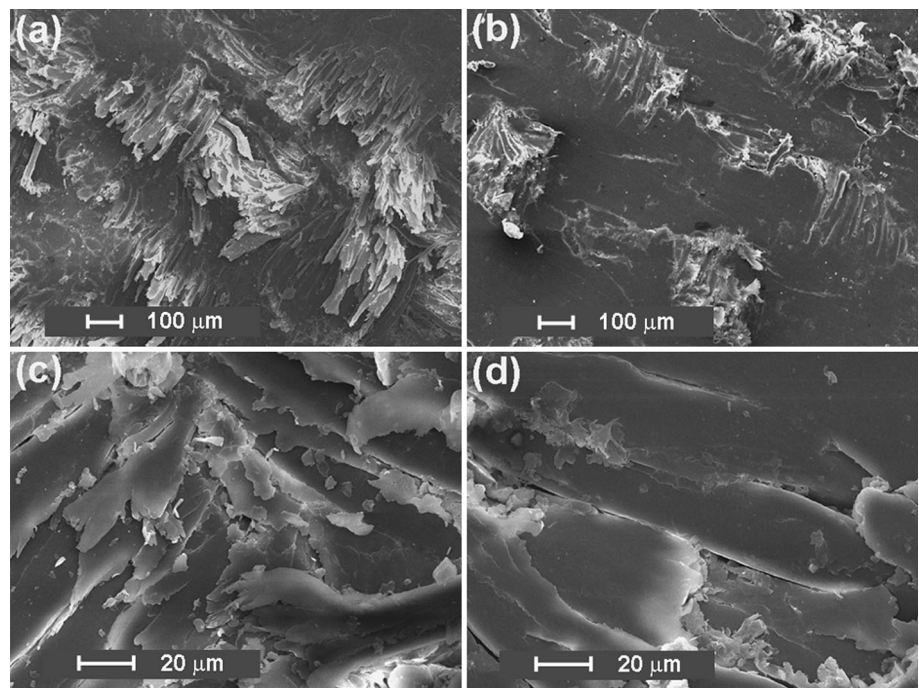


**Fig. 9** SEM images of the worn surfaces for a unfilled composite and b graphene oxide filled fabric composite at the sliding speed of 0.52 m/s, c, d magnified images of a, b, respectively. The applied load in the tests was 85 MPa



wear occurred on the surface. As shown in Fig. 6a, there are masses of furrows on the surface of the pin, and the transfer film is discontinuous and very thin. It was indicated that the counterpart pin underwent scratching during the sliding wear against the rough worn surface of the fabric composite. For 4 wt% graphite filled fabric composite, the amount of exposed fiber and fiber cut-off was less than that of the unfilled composite (see Fig. 5b, f). A more continuous transfer film can be seen on the counterpart pin, and the damage caused by abrasive wear is much milder (see Fig. 6b). When 2 wt% graphene was filled into the fabric composite, the worn surface of this composite was much smoother with little exposed and cut-off fibers (see Fig. 5c, g). Correspondingly, the counterpart pin is well protected by the uniform and continuous transfer film (see Fig. 6c). As for the 2 wt% GO reinforced fabric composite, the worn surface is the smoothest among the

fabric composites, with scarcely any exposed and cut-off fiber (see Fig. 5d, h). GO transferred onto the counterpart pin and formed a uniform and continuous transfer film (see Fig. 6d) [28]. To sum up, fillers reinforced composites exhibit improved antiwear property and load carrying capacity owing to the self-lubrication of the lubricants and the more continuous transfer film on the counterpart pin, especially for 2 wt% GO reinforced composite.

Since 2 wt% GO filled fabric composite exhibited the favorable antiwear property, the wear behavior of unfilled and 2 wt% GO filled fabric composite was further investigated under an increased load of 105 MPa. From the SEM image in Fig. 7a, it can be seen that large amount of fibers were cut off from the composite and most adhesive detached from the worn surface. Comparatively, much less fibers were cut down from the worn surface and large area of the worn surface was smooth for 2 wt% GO filled fabric

composite (see Fig. 7b). That is, the antiwear property of 2 wt% GO filled fabric composite was also reinforced under higher applied load.

The effect of sliding speed on the tribological properties of the composite

We next investigated the effect of sliding speed on the friction coefficients and wear rates of pure and 2 wt% GO filled fabric composites. As shown in Fig. 8a, the friction coefficient of pure composite was close to that of 2 wt% GO filled composite at all the sliding speeds investigated. However, the wear rate of 2 wt% GO filled composite was much lower than that of the pure composite at all the sliding speeds investigated. Moreover, the wear rate of 2 wt% GO filled composite varied in a small range with the sliding speed. It is proposed that fatigue wear and adhesive wear dominated the abrasion of the two fabric composites at low sliding speed. When the temperature of the worn surfaces went up to a certain amount owing to sliding speed increasing, the adhesive was softened and then the surface of the composite was polished during the sliding wear test, which resulted in the firstly decreased wear rate. However, the overabundant friction heat caused the decomposition of the adhesive and the reduction of mechanical property and antiwear property of the composite [29].

Figure 9 shows the worn surfaces of unfilled and GO filled hybrid fabric composites under the same sliding condition tested. For unfilled composite, bundles of fibers were cut down from the worn surface, indicating that severe fatigue wear occurred on the fabric composite surface (see Fig. 9a, c). On the contrary, GO filled fabric composite underwent milder damage, evidenced by much smoother worn surface and fewer exposed and cut-off fibers (see Fig. 9b, d). It is proposed that the self-lubrication of GO and easy-formed transfer film on the counterpart pin effectively reduced the wear loss of 2 wt% filled fabric composite at all sliding speeds tested.

## Conclusions

Graphite, graphene, and GO were employed as fillers to improve the tribological property of the hybrid PTFE/Nomex fabric/phenolic composite. Sliding wear tests showed that the antiwear property and load carrying capacity of 4 wt% graphite filled, 2 wt% graphene filled, and 2 wt% GO filled fabric composite were all improved, especially for the 2 wt% GO filled fabric composite, when compared with the unfilled fabric composites. For filler-reinforced fabric composites, GO reinforced fabric composite exhibited the highest bonding and tensile strength. It is believed that the favorable mechanical properties of the GO reinforced

fabric composite, the self-lubrication of GO, and the uniform and continuous film formed on the counterpart pin contributed cooperatively to the optimized tribological property of the fabric composite.

**Acknowledgements** The authors acknowledge the financial support of the National Science Foundation of China (Grant Nos. 51375472 and 51305429).

## References

- Sarasini F, Tirillò J, Valente M, Valente T, Cioffi S, Iannace S, Sorrentino L (2013) Effect of basalt fiber hybridization on the impact behavior under low impact velocity of glass/basalt woven fabric/epoxy resin composites. *Composites A* 47:109–123
- Thanomsilp C, Hogg PJ (2009) Penetration impact resistance of hybrid composites based on commingled yarn fabrics. *Compos Sci Technol* 63:467–482
- Wan YZ, Huang Y, He F, Li QY, Lian JJ (2007) Tribological properties of three-dimensional braided carbon/Kevlar/epoxy hybrid composites under dry and lubricated conditions. *Mater Sci Eng A* 452–453:202–209
- Xiang DH, Shu WC, Li K (2008) Friction and wear behavior of a new 40Cr steel-PTFE fabric composite under heavy loads. *Mater Sci Eng A* 483–484:365–368
- Villar-Rodil S, Paredes JI, Martínez-Alonso A, Tascón JMD (2001) Atomic force microscopy and infrared spectroscopy studies of the thermal degradation of Nomex aramid fibers. *Chem Mater* 13:4297–4304
- Khedkar J, Negulescu I, Meletis EI (2002) Sliding wear behavior of PTFE composites. *Wear* 252:361–369
- Aderikha VN, Shapovalov VA (2011) Mechanical and tribological behavior of PTFE-polyoxadiazole fiber composites. Effect of filler treatment. *Wear* 271:970–976
- Leal AA, Deitzel JM, McKnight SH, Gillespie JW Jr (2009) Interfacial behavior of high performance organic fibers. *Polymer* 50:1228–1235
- Shivamurthy B, Bhat KU, Anandhan S (2013) Mechanical and sliding wear properties of multi-layered laminates from glass fabric/graphite/epoxy composites. *Mater Des* 44:136–143
- Sharma M, Bijwe J (2012) Surface designing of carbon fabric polymer composites with nano and micron sized PTFE particles. *J Mater Sci* 47:4928–4935. doi:10.1007/s10853-012-6367-5
- Liu P, Huang T, Lu RG, Li TS (2012) Tribological properties of modified carbon fabric/polytetrafluoroethylene composites. *Wear* 289:17–25
- Sharma M, Bijwe J (2012) Influence of molecular weight on performance properties of polyethersulphone and its composites with carbon fabric. *Wear* 274–275:388–394
- Zhang XR, Pei XQ, Zhang JP, Wang QH (2009) Effects of carbon fiber surface treatment on the friction and wear behavior of 2D woven carbon fabric/phenolic composites. *Colloids Surf A* 339:7–12
- Zhang HJ, Zhang ZZ, Guo F (2010) A study on the sliding wear of hybrid PTFE/Kevlar fabric/phenolic composites filled with nanoparticles of TiO<sub>2</sub> and SiO<sub>2</sub>. *Tribol Trans* 53:678–683
- Zhang HJ, Zhang ZZ, Guo F (2012) Tribological behaviors of hybrid PTFE/Nomex fabric/phenolic composite reinforced with multiwalled carbon nanotubes. *J Appl Polym Sci* 124:235–241
- Shen XJ, Pei XQ, Fu SY, Friedrich K (2013) Significantly modified tribological performance of epoxy nanocomposites at very low graphene oxide content. *Polymer* 54:1234–1242
- Ren GN, Zhang ZZ, Zhu XT, Ge B, Guo F, Men XH, Liu WM (2013) Influence of functional graphene as filler on the



- tribological behaviors of Nomex fabric/phenolic composite. *Composites A* 49:157–164
18. Compton OC, Nguyen ST (2010) Graphene oxide, highly reduced graphene oxide, and graphene: versatile building blocks for carbon-based materials. *Small* 6:711–723
  19. Wan CY, Chen BQ (2012) Reinforcement and interphase of polymer/graphene oxide nanocomposites. *J Mater Chem* 22:3637–3646
  20. Hummers WS, Offeman RE (1958) Preparation of graphitic oxide. *J Am Chem Soc* 80:1339
  21. Xu YX, Bai H, Lu GW, Li C, Shi GQ (2008) Flexible graphene films via the filtration of water-soluble noncovalent functionalized graphene sheets. *J Am Chem Soc* 130:5856–5857
  22. Guo F, Zhang ZZ, Zhang HJ, Liu WM (2009) Effect of air plasma treatment on mechanical and tribological properties of PBO fabric composites. *Composites A* 40:1305–1310
  23. Hsiao MC, Liao SH, Yen MY, Liu PI, Pu NW, Wang CA, Ma CC (2010) Preparation of covalently functionalized graphene using residual oxygen-containing functional groups. *ASC Appl Mater Interfaces* 2(11):3092–3099
  24. Gao HJ, Zhang SH, Lu F, Jia H, Zheng LQ (2012) Aqueous dispersion of graphene sheets stabilized by ionic liquid-based polyether. *Colloid Polym Sci* 290:1785–1791
  25. Gonçalves G, Marques PAAP, Barros-Timmons A, Bdkin I, Singh MK, Emami N, Grácio J (2010) Graphene oxide modified with PMMA via ATRP as a reinforcement filler. *J Mater Chem* 20:9927–9934
  26. Liu P, Lu RG, Wang HY, Huang T, Li TS (2012) The mechanical and tribological properties of aramid (Twaron) fabric/polytetrafluoroethylene composites. *J Macromol Sci Phys* 51:1693–1704
  27. Zhang XR, Pei XQ, Wang QH (2011) Study on the friction and wear behavior of surface-modified carbon nanotube filled carbon fabric composites. *Polym Adv Technol* 22:2157–2165
  28. Li YQ, Wang QH, Wang TM, Pan GQ (2012) Preparation and tribological properties of graphene oxide/nitrile rubber nanocomposites. *J Mater Sci* 47:730–738. doi:[10.1007/s10853-011-5846-4](https://doi.org/10.1007/s10853-011-5846-4)
  29. Su FH, Zhang ZZ, Guo F, Song HJ, Liu WM (2006) Tribological properties of the composites made of pure and plasma treated-Nomex fabrics. *Wear* 261:293–300